SILICON NANOWIRES: CONDITION OF SYNTHESIS AND SIZE SELECTION

C. Benoit, S. Bastide, C. Lévy-Clément*

Institut de Chimie et des Matériaux Paris Est, CNRS-UMR 7182
2-8, rue Henri-Dunant 94320 Thiais, France
* levy-clement@icmpe.cnrs.fr; Tel: 33 1 49 78 13 31; Fax: 33 1 49 78 12 03

ABSTRACT: Silicon nanowires were obtained by metal-assisted chemical etching. Two different top-down methods were used: (i) a one-step method using HF/AgNO$_3$ solution, in which Ag is both the oxidant and the catalyst; (ii) a multi-step method including masking with a monolayer of polystyrene spheres; a metallization step by Ag electroless deposition or Au evaporation; and finally etching in HF/H$_2$O$_2$. The effects of temperature, reactant concentrations and silicon resistivity were studied and a formation mechanism proposed for the one-step method.
Keywords: etching, silicon nanowires, tandem

1 INTRODUCTION

The all-silicon (Si) tandem cell is a third generation solar cell concept relying on the use of a top cell made of nano-structured Si having a higher band gap than bulk Si (i.e. 1.7 eV) [1]. Quantum confinement is therefore needed and Si quantum dots embedded in a transparent and insulating matrix are widely investigated for that purpose. Alternative to a full 3D confinement, a 2D confinement is also efficient for increasing the band gap and present some advantages over quantum dots (i.e. conductivity, contacts). It can be obtained with Si nanowires (SiNWs), providing their diameters are below 3.5 nm [2]. SiNW synthesis is generally performed in a bottom-up approach using the vapor-liquid-solid method [3]. In this paper, we are investigating a top-down alternative route based on electroless metal-assisted Si etching to obtain well aligned SiNW arrays [4]. Basically, a noble metal is deposited on the surface in the form of nanoparticles which act as catalysts for Si etching in HF solutions containing an oxidizing agent. As a consequence, etching only occurs at the level of the metal nanoparticles and results in the formation of well defined mesopores (20-100 nm in diameter). The case presented is Ag nanoparticles or a Au layer as metal catalysts.

2 EXPERIMENTAL

Si substrates. Polished (100) p-type (B-doped) c-Si wafers with a resistivity of 1-3 Ω.cm were cleaved into 1×1 cm^2 samples. The Si surface morphology was investigated using a Leo 1530 Scanning Electron Microscope (SEM) with a GEMINI field emission electron gun.

Chemicals. All chemicals were purchased from Prolabo. The solutions were prepared from 40 wt.% HF, 30 wt.% H$_2$O$_2$, AgNO$_3$ (Rectapur) and 18.2 MΩ.cm ultra-pure H$_2$O. Chemical treatments were performed under carefully controlled temperature using a Huber Ministat 240 cryothermostat.

AgNO$_3$/HF etching. The initial experimental conditions were 5 M HF, 0.02 M AgNO$_3$ with etching performed during 1 h at 50°C [5]. Parameters were changed to observe the effect of each. After etching, the samples were rinsed several times with deionized water and sonicated during 1 min to remove most of Ag.

Polystyrene (PS) sphere mask. PS spheres were deposited by spin coating with a Spin150 from APT. The Si surface was made hydrophilic as followed: Si wafers were washed in acetone and ethanol, then ultrasonicated for 10 minutes in a piranha solution (4:1 (v/v) H$_2$SO$_4$/H$_2$O$_2$). Colloidal dispersions of spheres, 1 µm in diameter, were prepared from Alfa Aesar commercial solutions (2.5 wt.%). Sphere dispersions were centrifuged and diluted to obtain the following composition: 10/60/15/15 in volume of PS/ethanol/H$_2$O/ethylene glycol (PS/EtOH/H$_2$O/EG). An ordered monolayer of spheres was obtained by spreading 50 µL of a prepared dispersion on a 1 x 1 cm² Si substrate and rotating at ω = 3000 rpm. Annealing at 110°C during 30 min was performed to have cohesion between the spheres.

Metallization. Ag was deposited via an electroless method on the PS coated Si surface in a AgNO$_3$/HF solution during 5 min with [AgNO$_3$] = 0.5 mM and [HF] = 0.15 M.

Au layers were deposited using a thermal evaporator at a pressure lower than 5.10^{-6} Pa.

Chemical etching was then performed in HF/H$_2$O$_2$ solution at 28°C.

3 RESULTS AND DISCUSSION

3.1 SiNW Formation in a One-Step Process

Metal assisted etching is based on a galvanostatic reaction between an oxidizing agent and Si. In this case, the cathodic reaction is the reduction of Ag$^+$, according to:

$$Ag^+ \rightarrow Ag + h^+ \qquad E_0 = + 0.79 \text{ V/NHE}$$

The anodic reaction is the chemical dissolution of Si which can be presented in the following general form:

$$Si + 6HF + nh^+ \rightarrow H_2SiF_6 + nH^+ + \left(\frac{4-n}{2}\right)H_2$$

where n is the number of holes per dissolved Si atom.

Depending on the experimental conditions, the dissolution regime and n can change. At low HF concentration or high oxidizing agent concentration, SiO$_2$ forms at the surface and is slowly solubilized by HF, $n = 4$ with no H$_2$ evolution (polishing regime). At high HF concentration or low oxidizing agent concentration, dissolution occurs with $n = 2$ to 3, corresponding to 1 to 0.5 H$_2$ evolved per dissolved Si atom (porous Si formation regime) [6, 7].

The role of Ag is to catalyze the Si dissolution by both collecting electrons (locally) from Si and allowing Ag^+ ions to be reduced at its surface. The formation of Ag/Si Schottky junctions favors local etching near the Ag nanoparticles, hence the formation of vertical cylindrical mesopores. The unetched walls between the mesopores constitute the nanowires (Fig. 1).

In order to obtain SiNWs with optimized length and diameter, we carried out a systematic study by varying several etching parameters: [AgNO$_3$], [HF] and temperature. The initial experimental conditions were 5 M HF, 0.02 M AgNO$_3$ with etching performed during 1 h at 50°C [5]. With respect to the initial values, the concentrations were varied by a factor two (lower or higher) and the temperature by plus or minus 20°C.

SiNWs are obtained under all tested conditions. Using the initial conditions (Fig. 1d), SiNWs 35 µm long with diameters between 30 to 100 nm are formed.

We observed that the SiNW length depends on the temperature: 20 µm at 30°C and 55 µm at 70°C (Fig. 1 *a→e)*. It also depends on [HF]: 24 µm at 2.5 M and 67 µm at 10 M HF (Fig.1 *b→f)*. The diameters of SiNWs are not highly modified but we can notice that SiNWs are more compact and less detached for 10 M HF. Increasing [HF], Si amount in the SiNWs layer increases.
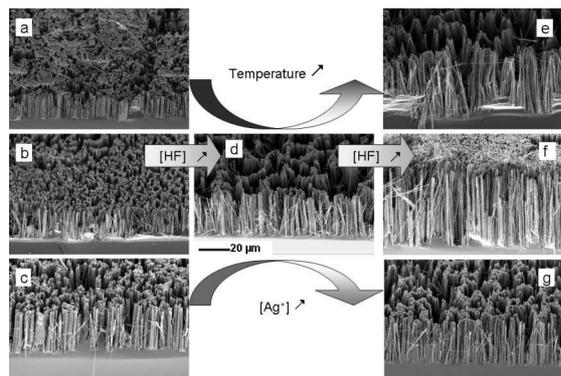

Figure 1: SEM images of SiNWs obtained by metal-assisted etching: (d) initial conditions; (a→e) increasing temperature; (b→f) increasing [HF]; (c→g), increasing [AgNO$_3$].

Surprisingly, a higher [AgNO$_3$] (Fig. 1 *c→g)* does not affect the length (35 µm) but reduces the substrate thickness. For a even higher [AgNO$_3$], the thickness of the Si wafer is reduced from 380 to 100 µm (Fig. 2 – note that in Fig. 2b both sides of the Si wafer are visible). The diameter of the nanowire has increased, as most of the nanowires are columnar with a rougher surface.
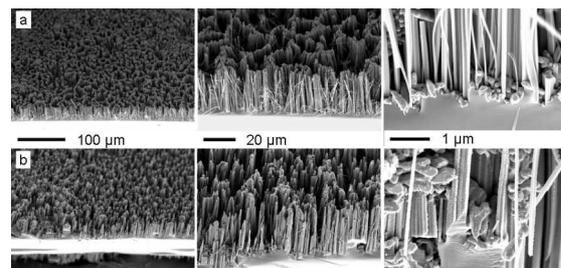

Figure 2: SEM images of SiNWs obtained for different [AgNO$_3$]: (a) 0.02M; (b) 0.2M.

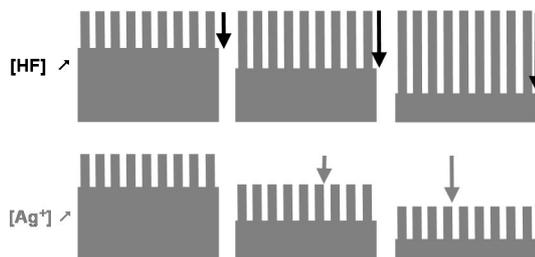A schematic representation of the effect of [HF] and [AgNO$_3$] is shown in Fig. 3.

Figure 3: Schematic representation of the effect of [HF] and [AgNO$_3$] on SiNW formation.

The formation mechanism of the SiNWs can be explained by the catalytic effect of the Ag nanoparticles generated in situ. As observed in classical metal assisted etching in HF/oxidant solutions, the dissolution occurs at the level of Si/metal contacts [5, 7]. Indeed, from the SEM image of the SiNW/Si interface in Fig. 4b, it is clear that the Ag deposit shape determines the morphology of the wire at the nm scale.
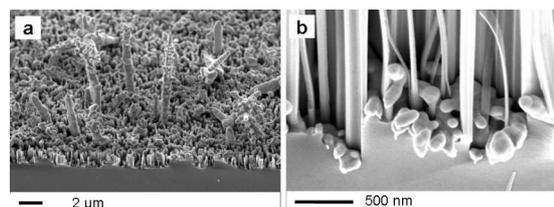

Figure 4: SEM images of Si surface (a) after 1 min Ag deposition and (b) after 1 h, high magnification of the bottom of SiNWs.

First, isolated Ag nanoparticles are deposited on the Si surface; their growth is only limited by Ag^+ diffusion. Concomitantly, they penetrate into bulk Si and some nanoparticles connect to others. Because of the Ag^+ diffusion regime from the solution bulk to the Si surface, further Ag deposition results in the growth of dendrites (Fig. 4a) which are eventually visible as Ag sponge around the sample. During etching, oxidation of Si occurs at the bottom of the Ag network while reduction of Ag^+ occurs at its top. As it grows, the Ag network sinks into the Si substrate.

The effect of [HF] on the nanowire length is surprising since in the experiments (Fig. 1 b→f) [AgNO$_3$] (fixed at 0.02 M) is much lower than [HF] (2.5 - 10 M), and should therefore set the dissolution rate (at a constant value). At the same time, the SEM images of samples etched at [HF] = 10 M (i.e. with the longest SiNWs) show that the surface structures are closer to wire bundles or corrugated walls (Fig. 1f) than the SiNWs observed at lower [HF]. This indicates that the Ag/Si contact area (bottom of the Ag network) is reduced when [HF] is increased. We hypothesize that [HF] may influence the deposition of Ag at the initial stage of the process (nucleation step), hence the extent of the Si/Ag contact area. Because Si is dissolved only at Ag/Si contacts, different contact areas could result in different SiNW lengths, even if the dissolution rate and etching time are identical.

Increasing [AgNO$_3$] results in a higher etching rate, as expected, and full dissolution of the substrate rather than in longer SiNWs (cf. Fig. 3). SEM observations of sample etched for 1 min, shows that the surface stays flat although the weight loss corresponds to an etched thickness of 6 µm. We assume that at the first stage of etching, consumption of Ag$^+$ is not controlled by diffusion, and as a consequence a "polished" surface is obtained. The duration of this stage, hence the thinning of the substrate, increases with [AgNO$_3$]. Once the surface is Ag$^+$ depleted, i.e. the Ag$^+$ diffusion regime is reached, SiNWs start to grow. After 5 min etching, Si wires 200 nm in length are observed (while 29 µm of Si were etched away).

Besides SiNWs, various kinds of columnar Si structures are formed, irrespective of the bath composition. The shape of the Si structures is dictated by that of the dendrites-like Ag-deposits, connected in a Ag network, which itself is not too sensitive to the different conditions we have tested.

3.2 SiNW Formation in a Multi-Step Process

Because in HF/AgNO$_3$ the deposition of Ag particles is difficult to control, a mask could be useful to protect Si areas around which metal could be deposited [8].

PS spheres were assembled on the surface by spin coating at 3000 rpm using a dispersion of PS sphere/EtOH/H$_2$O/EG (10:60:15:15 in volume). These conditions lead to a compact monolayer of PS spheres, on almost the entire surface. (Fig. 5a) PS spheres can be easily removed by sonication.

3.2.1 Ag metallization by electroless deposition.

Electroless Ag deposition is based on the galvanostatic reaction already mentioned above between Ag$^+$ and Si in HF aqueous solution. After 5 minutes in HF/AgNO$_3$, Ag nanoparticles are visible on the Si surface except at the level of Si/PS spheres contact areas (Fig. 5 b). Masked areas are 200 nm in diameter and display a hexagonal arrangement with spacing of 1µm (Fig. 5c and d).
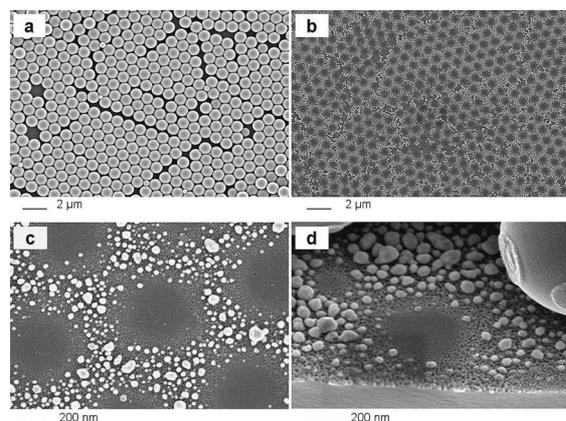

Figure 5: SEM images of (a) PS sphere monolayer; (b, c, d) electroless Ag deposit.

The presence of Ag nanoparticles catalyzes Si etching. As with Ag$^+$/HF solution, Ag collects electrons from Si and acts as a microcathode for the reduction of the oxidant, H$_2$O$_2$. The anodic reaction is the oxidation of

Si, already presented in section 3.1, and the cathodic reaction is the reduction of H$_2$O$_2$, according to:

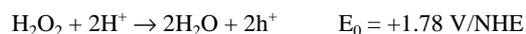$$H_2O_2 + 2H^+ \rightarrow 2H_2O + 2h^+ \qquad E_0 = +1.78 \text{ V/NHE}$$

Fig. 6a shows a SEM cross section image of an etched sample under the conditions reported in Table 1a. The formation of SiNWs is not observed. A close inspection indicates that the Ag particles migrate in the <100> direction (perpendicularly to this Si surface) but also randomly in other directions [9]. This results in etching under masked areas, and poor efficiency of the Ag metallic replica-mask obtained by electroless deposition.

We tried to address this issue first by changing the SI resistivity (ρ) and HF-H$_2$O$_2$ concentration in order to favor migration of the Ag nanoparticles in the <100> direction. The different sets of experimental conditions are summarized in Table 1(b-d).

Table 1: Experimental conditions of etching in HF/H$_2$O$_2$ for Ag metallized samples. In all cases, the etching time is 5 min at 28°C.

	[HF] (mol.l^{-1})	[H$_2$O$_2$] (mol.l^{-1})	ρ (ohm.cm)
a	18	2	1-3
b	4.5	0.5	1-3
c	4.5	0.5	10-15
d	2.5	0.625	10-15

The SEM cross section images of etched samples b, c and d are shown in Fig. 6(b-d).

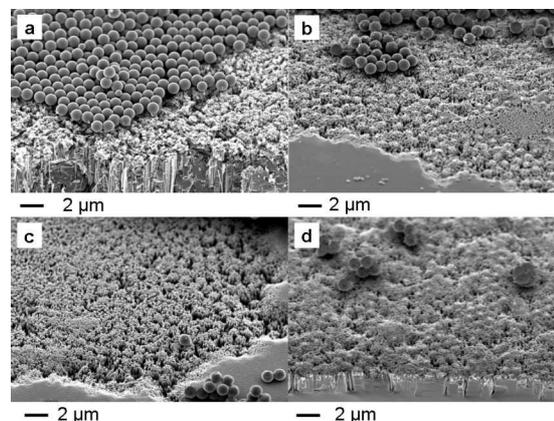**Figure 6:** SEM images of samples etched under the different sets of conditions reported in Table 1.

We observe that decreasing [HF] and [H$_2$O$_2$] (at a constant ratio) favors migration in the <100> (Fig. 6a and b). Using Si substrates of higher resistivity has the same effect (Fig. 6c). Increasing the HF/H$_2$O$_2$ concentration ratio (at constant [HF]) also favors perpendicular migration (Fig. 6c and d). However, changing the etching conditions was not sufficient to obtained well defined SiNWs.

As a second option, we tried to deposit more Ag between the spheres in order to obtain complete etching of these regions. This was performed by increasing [Ag$^+$] during the metallization step from 0.5 mM to 5 mM. In this way, more Ag was deposited between the spheres, but still in the form of isolated Ag particles with a large dispersion in size and etching led to the same lack of

masking effect due to their migration in random directions.

3.2.2 Au metallization by evaporation.

A Au film 15 nm thick is deposited on the Si surface masked with PS spheres. The spheres are not damaged by the thermal deposition process and the non coated areas exhibit the diameter of the spheres (cf. Fig. 7a). The Au replica mask is well defined, free of holes and with sharp edges.

Etching in HF/H_2O_2 using the Au replica-mask as a catalyst was performed in 2.5 M HF and 0.63 M H_2O_2 for 5 min. The Si surface in contact with the Au layer is completely dissolved. Si pillars are obtained below the spheres, with approximately the same diameter as that of the sphere (Fig. 8b). The pillars are perpendicular to the (100) oriented surface.
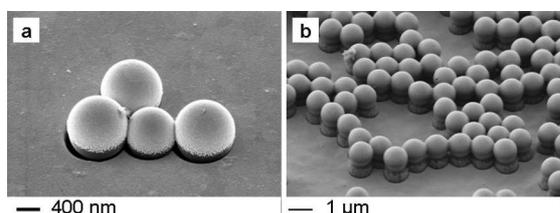

Figure 7: SEM images of a Si surface after (a) thermal evaporation of Au and (b) HF/H_2O_2 etching.

At high magnification, the SiNW walls appear rough, especially at their top. This could be due to the grainy nature at the nm level of the evaporated Au layer edges or to the porous Si formation resulting from the polarization of the Si sample contacted by the Au layer. In this latter case, the rougher aspect of the SiNW at its top would result from the longer etching time it experiences.

4 CONCLUSION

The formation of SiNWs by a one-step method based on metal assisted chemical etching has been investigated. We found that [HF] and the temperature are two key parameters that allow monitoring the SiNWs length. The nanowire diameter and density depend on the Ag deposit shape (Ag network). A mechanism for the formation of SiNWs and Ag network was proposed: Si dissolution occurs where Si is in direct contact with Ag (catalytic effect), i.e. at the bottom of the Ag network. The top of this network grows in the form of dendrites as Ag^+ is further reduced. From an electronic point of view, electrons injected at the bottom of the Ag network (Si oxidation) are consumed at the top (reduction of Ag). This one-step method suffers however from the lack of control of the Ag network shape even when controlling etching parameters such as the concentration of reactants or the bath temperature.

The formation of SiNWs using a multi-step method including masking the surface by PS spheres and metallization by electroless deposition of Ag or evaporation of a Au film has also been investigated. In the former case, the electroless technique results in the deposition of individual Ag nanoparticles. During Si etching in HF/H_2O_2, the majority of the Ag nanoparticles migrates perpendicularly to the surface into the Si wafer, however some of them migrate in random directions

(even under protected areas), which strongly limits the replica mask efficiency. In the latter case, the use of a cohesive metal layer (Au) solves this problem and allow to obtain in a controlled fashion SiNWs with diameter corresponding to that of the PS spheres (1 µm). The next step of our work will be to use smaller spheres to obtain narrower Si wires.

REFERENCES

[1] E.-C. Cho and al, Advances in OptoElectronics, vol 2007, Article ID 69578

[2] L.T. Canham, Applied Physics Letters 57, 1046 (1990)

[3] Kok-Keong Lew et al., Applied Physics Letters 85, 3101 (2004)

[4] K.-Q. Peng, Y.-J. Yan, S.-P. Gao, Adv.Mater. 14, No.16 (2002), 1164-1167

[5] K. Peng, H. Fang, J. Hu, Y. Hu, J. Zhu, Y. Yan, S. Lee, Chem. Eur. J. (2006) 12, 7942-7947

[6] E.S. Kooij, K. Butter and J.J. Kelly, Electrochem. and Solid-State Lett., 2(4) 178-180 (1999)

[7] C. Chartier, S. Bastide, C. Lévy-Clément, Electroch. Acta 53 (2008) 5509-5516

[8] S. Ono, A. Oide, H. Asoh, Electrochim. Acta, 52 (2007) 2898-2904

[9] K. Tsujino, M. Matsumura, Electrochim. Acta 53 (2007) 28-34